SweepSAR: Beam-forming on Receive using a Reflector-Phased Array Feed Combination for Spaceborne SAR

A. Freeman, G. Krieger[2], P. Rosen, M.Younis[2], W. T. K. Johnson, S. Huber[2], R. Jordan[1], A. Moreira[2]

1. Jet Propulsion Laboratory, California Institute of Technology, 4800 Oak Grove Drive, Pasadena, CA 91109, USA. e-mail: Anthony.freeman@jpl.nasa.gov, Tel: (818) 354 1887
2. Microwaves and Radar Institute (HR), German Aerospace Center (DLR), 82234 Wessling, Germany.

At present, spaceborne synthetic aperture radars (SARs) can only cover wide swaths using techniques such as ScanSAR, which involves trade-offs in resolution or number of looks; or TOPS-SAR, which also requires an advanced phased array antenna capable of steering in azimuth. Performance in either case is limited by signal-to-noise considerations and by range ambiguities. Digital beam-forming techniques have been proposed that offer high-resolution and wide swaths, but generally require complex beam-forming networks, large phased array antennas (especially at longer wavelengths), very high data rates and/or onboard processing to succeed. All these stretch currently available technologies to their limit.

In this paper, an alternative approach is described that is suited for longer wavelength SARs in particular, employing a large, deployable reflector antenna and a much simpler phased array feed. To illuminate a wide swath, a substantial fraction of the phased array feed is excited on transmit to sub-illuminate the reflector. Shorter transmit pulses are required than for conventional SAR. On receive, a much smaller portion of the phased array feed is used to collect the return echo, so that a greater portion of the reflector antenna area is used. The locus of the portion of the phased array used on receive is adjusted using an analog beam steering network, to ‘sweep’ the receive beam(s) across the illuminated swath, tracking the return echo. This is similar in some respects to the whiskbroom approach to optical sensors, hence the name: SweepSAR.

SweepSAR has advantages over conventional SAR in that it requires less transmit power, and if the receive beam is narrow enough, it is relatively immune to range ambiguities. Compared to direct radiating arrays with digital beam-forming, it is much simpler to implement, uses currently available technologies, is better suited for longer wavelength systems, and does not require extremely high data rates or onboard processing.

I. Introduction

Conventional SAR systems suffer from limitations in swath width and resolution: generally one cannot have both wide swath coverage and high resolution [1]. In designing SAR systems, one usually has some trade-off between the two, because the limited antenna dimensions constrain the trade space [2]. ScanSAR techniques allow wider swaths employing a burst mode of data acquisition, with the radar beam pointed electronically to different subswaths in elevation [3], [4]. ScanSAR achieves wider swath at the expense of degraded azimuth resolution or fewer looks. It was first demonstrated on NASA/JPL’s SIR-C mission in 1994 [5] and was one of several key techniques that enabled the follow-on SRTM mission to successfully measure more than 80% of the Earth’s topography [6], [7].

More recently, an innovative approach to SAR data acquisition, named TOPS-SAR, has been proposed by De Zan and Guarnieri [8]. TOPS-SAR includes burst-mode operation, scanning of the antenna footprint in azimuth during each burst, and elevation steering to illuminate different subswaths. It involves the same trade-offs between azimuth resolution/number of looks and swath width as ScanSAR, but offers significantly improved radiometric and ambiguity performance. This is achieved at the expense of increased complexity – TOPS-SAR requires beam steering in both elevation and azimuth, which can only be done in practice using a sophisticated, two-dimensional, phased array antenna.

In order to overcome the fundamental limitations of conventional SAR systems, several innovative designs have been suggested where the receiving antenna is split into multiple sub-apertures that are connected to individual receiver channels. One promising approach is the displaced phase centre antenna (DPCA) technique which employs multiple apertures in the along-track direction to acquire for each transmitted pulse additional samples along the synthetic aperture. As a result, one may reduce the transmit PRF without elevating the azimuth ambiguities. The DPCA technique therefore enables a decoupling of the otherwise contradicting requirements for wide swath coverage and high azimuth resolution [4].

An extension of the DPCA technique is the Quad Array system [21] that uses additional apertures in elevation to suppress range ambiguous returns [22]. By this, it becomes possible to further increase the image swath, but the drawback is a range gap in the middle of the wide swath since it is impossible to simultaneously transmit and receive radar pulses. A further extension of the DPCA technique is the High-Resolution Wide-Swath (HRWS) SAR [23][13]. This system combines a separate small transmit antenna with a large receiver array. The small transmitter illuminates a wide swath on the ground and the large receiver array compensates for the inevitable Tx gain loss by a real-time digital beamforming (DBF) process in elevation denoted as scan-on-receive (SCORE). According to SCORE, the receiver beam is moved in synchrony with the apparent motion of the transmitted pulse along the ground, such that the maximum antenna gain can be used at all times. The origin of this idea can be traced back to the patent of J. Blythe [24] and the SCORE technique has been further elaborated in [9], [10], [25] and [26]. The HRWS system uses in addition multiple azimuth channels to image a wide swath without rising ambiguities. The combination of the azimuth signals from the multiple apertures requires the application of dedicated multi-channel SAR signal processing algorithms as introduced in [19] and further detailed in [20]. More recently, the approach has been demonstrated on a ground-based SAR testbed [11].

An elegant extension of DBF, involving the transmission of multiple waveforms was proposed by Krieger et al [12]. Their modified approach to DBF SAR offers improved ambiguity performance at the expense of increased complexity in data acquisition and processing.

Note that most of these techniques for wide swath, high resolution imaging using DBF or extensions are introduced in the context of short wavelength SAR systems, e.g. X-band or Ka-band. For conventional (stripmap) SAR at such short wavelengths, the antenna height is generally very small (typically around 12 wavelengths for an elevation beamwidth of 5-6 degrees, which illuminates ~ 100 km from low Earth orbit). Adding height to these small antennas to allow multiple receive apertures in elevation for DBF does not increase the overall antenna area to an unreasonable extent. In [13] for example the receive antenna dimensions for an X-band HRWS system are 12 m long by 1.66 m high.

The situation is dramatically different at longer wavelengths. Scaling the application of the HRWS approach in [13] to an L-band system would require an antenna of dimension 12m by 13.3m, which is four times bigger than the SIR-C L-band antenna. Mass/unit area capabilities for phased array antennas are in excess of 10 kg/sq. m, and they have to be deployed after packaging for launch in significantly smaller launch vehicle shrouds. Deployment of antennas of this size/mass in space requires heavy lift capacity and robust spacecraft attitude control, as well as elaborate deployment mechanisms. Such large, massive antennas must, therefore, be considered technically challenging.

In summary, digital beam-forming approaches for SAR seem well-suited to improve performance for shorter wavelength (C-, X-, or Ka-band) SAR systems. DBF SAR approaches result in system designs with reduced power levels, mode flexibility, wider swath width, better spatial resolution and lower ambiguity levels. But they typically have complex beam-forming networks, very high data rates, increased operational complexity, and require onboard processing capability. At longer wavelengths, DBF SAR approaches result in very large, heavy phased array antennas, which present several technical challenges to deploy in space. There is a need for a beam-forming approach that provides most of the advantages of DBF SAR without the disadvantages, particularly at longer wavelengths.

In this paper, we present such an approach, termed SweepSAR, which uses a lightweight, deployable reflector antenna combined with a simple, one-dimensional phased array feed. SweepSAR can be implemented as an analog beam-forming approach. In this case the entire swath is illuminated on transmit, while on receive, an analog beam-steering network excites the elements of the phased array feed in succession such that a pencil beam scans the swath, tracking the locus of the return echo.

In section II, we formulate some simple equations to characterize the performance of a SweepSAR system. These are developed from the corresponding equations for conventional SAR systems. In section III we show how the SweepSAR technique can yield lower peak and average transmit power requirements, or be used to generate wider swaths than conventional SARs. Finally in section IV we summarize our results and discuss their implications for future SAR missions, but especially the NASA/JPL DESDynI mission [14], and the corresponding Tandem-L mission proposed by both DLR and NASA/JPL[15].

II. SweepSAR Concept

Ramanujam et al [16] have patented a multi-beam reflector antenna with a simple beamforming network, primarily for scanning a pencil beam to various geographic locations for communications satellites in geosynchronous orbit. A beamforming network is used to excite a subset of an array of feed horns, to generate the required pencil beam steered to the required angle(s).

Here we study a unique adaptation of this approach to a spaceborne SAR in low earth orbit, first proposed by Blythe [24] and improved upon by Kare [25]. In following this approach, we use a large reflector antenna fed by a one-dimensional array feed. The basic concept is illustrated in Figure 1. The array feed is configured so that it allows beam steering in elevation. On transmit, multiple feed elements are used to sub-illuminate the reflector, which results in a wide illuminated swath on the ground. On receive, significantly fewer elements of the feed array are excited by the beam-forming network. This means that more of the large reflector is used on receive, so that the receive beam is shaped like a pencil beam. The locus of the portion of the phased array used on receive is adjusted in real-time across the feed array using an analog or digital beam steering network, to 'sweep' the receive beam across the illuminated swath, tracking the return echo. Though both analog and digital beam-forming can be used, it should be noted that the analog approach has distinct advantages of lower data rates and simpler implementation. On the other hand, an analog implementation imposes constraints on the maximum pulse duration and may additionally result in a substantial performance loss when compared to a digital feed system. The overall approach has similarities to the whiskbroom approach to optical sensors, hence the name: SweepSAR.

The SweepSAR approach differs from DBF SAR and its extensions in that its analog implementation only requires a single RF/digital receiver per radar channel, has a much lower data rate, and requires no onboard processing of data. The single receiver is fed only by the signals from the receive feed elements activated by the beam steering network at each point in time, so that one cannot

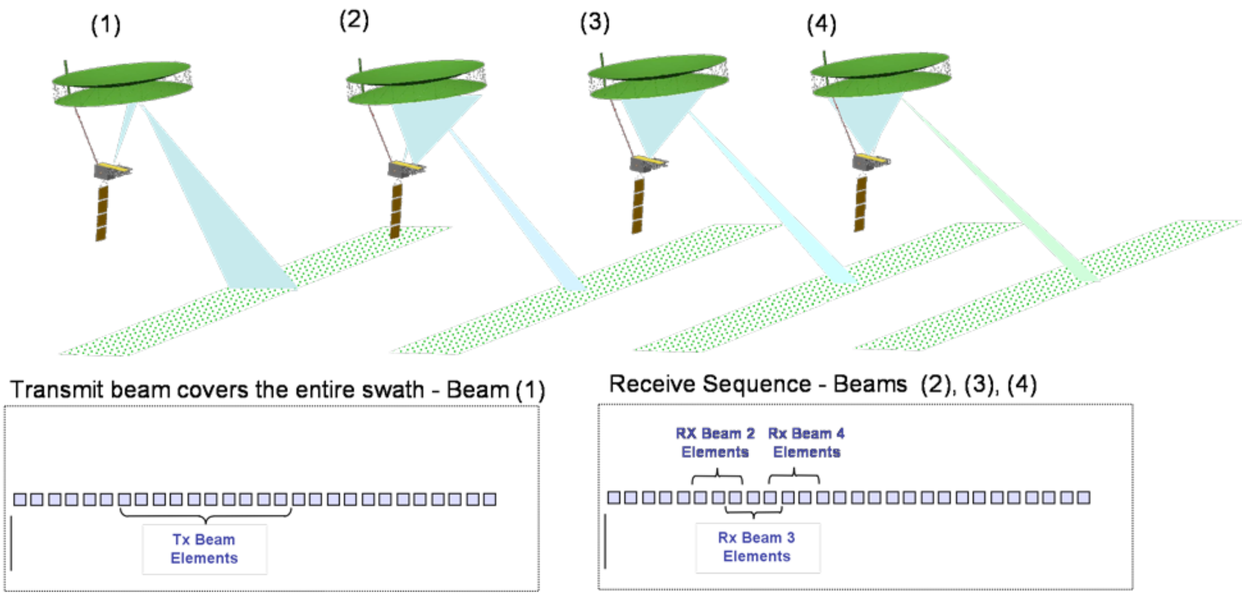

Figure 1: In SweepSAR mode the transmit beam illuminates the full, desired swath and the receive beams are 'swept' across the illuminated swath. Elements of the linear, phased array feed are selected to adjust the size and pointing of the transmit and receive beams.

reconstruct different receive beams from the acquired signals – thus we term this an analog beam-forming technique, rather than a digital beam-forming technique.

The imaging geometry for a SweepSAR system is illustrated in Figure 2, which for simplicity shows a planar array with smaller dimensions on transmit, and larger dimensions on receive.

To evaluate the benefits of the SweepSAR technique we introduce an appropriate form of the Signal-to-Noise Ratio (SNR) for this kind of system:

$$SNR \cong \left(\frac{P_t G^t G^r \lambda^2 L_s G_p}{(4\pi)^3 R^4}\right)\left(\frac{\sigma^o}{N_o}\right)\left(\frac{c\tau_p}{2\sin\theta_i}\right)\left(\frac{\lambda R}{L}\right)$$

(1)

where P_t is the transmit power, G^t is the antenna gain on transmit, G^r is the antenna gain on receive. L_s represents any system losses (and is < 1), and G_p any gain realized during processing (usually ~equal to 1). σ^o is the normalized radar cross section of the target area and N_o is the noise in the receiver channel. τ_p is the pulse length, c the speed of light, θ_i the incidence angle, λ the radar wavelength, R the range between the target and the radar an

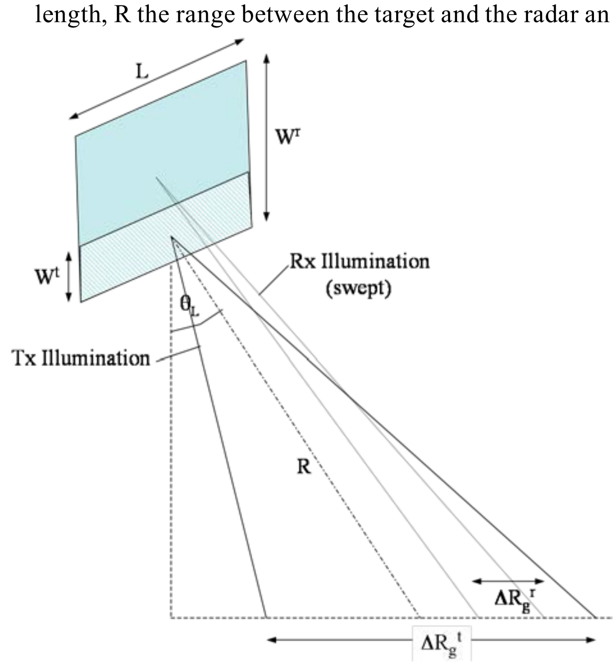

Figure 2: SweepSAR side-looking geometry

tenna, and L is the length of the antenna (in the along-track direction). The latter two terms in (1) represent the dimensions of the area from which backscattered energy is collected – when multiplied by the normalized radar cross section (RCS) or σ^o, it becomes the actual RCS measured in units of area.

Next we adopt a common approximation for the one-way gain of a planar array [1]:

$$G \cong \frac{4\pi A_e}{\lambda^2} \approx \frac{4\pi LW}{\lambda^2} \tag{2}$$

where A_e is the effective area of the antenna, and W is its height (cross-track dimension). Note that we will not generally be using planar arrays for SweepSAR, but for now they serve to illustrate the concepts at hand. We can now recast (1) for the beam center as:

$$SNR \cong \left(\frac{P_t L^t W^t L^r W^r L_s G_p}{(4\pi)\ \lambda^2 R^4}\right)\left(\frac{\sigma^o}{N_o}\right)\left(\frac{c\tau_p}{2\sin\theta_i}\right)\left(\frac{\lambda R}{L}\right) \tag{3}$$

where we have introduced the idea of having different dimensions for the transmit and receive antennas. Since we have no reason to make the antenna lengths (along-track dimension) different on transmit and receive, we can simplify (3) by setting $L^t = L^r = L$, to give:

$$SNR \cong \left(\frac{P_t L W^t L W^r L_s G_p}{(4\pi)\ \lambda^2 R^4}\right)\left(\frac{\sigma^o}{N_o}\right)\left(\frac{c\tau_p}{2\sin\theta_i}\right)\left(\frac{\lambda R}{L}\right) \tag{4}$$

Noting that the noise in the receiver can be expressed as:

$$N_o = kT_o F B_n \tag{5}$$

where k is Boltzmann's constant, T_o the receiver temperature, F the noise figure, and B_n the noise bandwidth, we can identify the degrees of freedom the radar designer has with a SweepSAR system by pointing out that:

$$SNR \propto \frac{P_t L W^t W^r \tau_p}{B_n} \tag{6}$$

which is the same as for a conventional SAR if one sets $W^t = W^r = W$. This assumes of course that the wavelength, incidence angle, target RCS and operating range are all pre-determined from the system requirements.

The average power on transmit for a SweepSAR system is given by the following expression:

$$P_t^{av}(DC) = \left(P_t\ \tau_p\ PRF\ D_c\right)/\varepsilon \tag{7}$$

where D_c is the radar duty cycle (percentage on-time per orbit) and ε is the efficiency of the conversion from DC to RF power by the high-power amplifiers used on transmit (typically in the range 0.3 to 0.4 for solid-state amplifiers). (7) represents the amount of power the spacecraft power system will have to supply to the radar system for transmission of RF pulses; added to that should be the amount of power used by the radar receiver and other electronics, but (7) is often the larger term, which therefore drives the amount of power needed for the radar payload from the solar panels (in a solar-powered spacecraft), and therefore the size of those panels. In later calculations we shall show estimates for the average power on transmit that assume a 100% duty cycle – these should be modified to reflect the actual percentage on-time for any given mission.

The swath width for a SweepSAR system is determined by the width of the illuminated swath projected onto the ground (assuming the entire swath is scanned on receive), which is given by:

$$\Delta R_g^t \cong \frac{\lambda R}{W^t \cos\theta_i} \tag{8}$$

An additional constraint for an analog feed SweepSAR system, one not normally considered for conventional stripmap SAR, is that the pulse length projected onto the ground should be less than the width of the 'swept' receive beam projected onto the ground, i.e.

$$\frac{c\tau_p}{2\sin\theta_L} < \frac{\lambda R}{W^r \cos\theta_i} \tag{9}$$

Given that we have fixed the antenna length in the along-track dimension, the lower limit for the PRF in a SweepSAR system is the same as for a conventional SAR system, i.e.

$$PRF > B_D \cong 2V/L \tag{10}$$

or a factor of two higher in quad-pol mode. B_D and V are the received Doppler bandwidth and the platform velocity, respectively. The upper limit for the PRF in a conventional SAR is set by the requirement to not have range ambiguous returns arrive from the illuminated swath at the same instant that a desired return is expected. It can be expressed as:

$$PRF < c/\left(2\Delta R_g^r \sin\theta_i\right) \tag{11}$$

where ΔR_g^r is the width of the recorded swath. In SweepSAR, the receive beam is generally much narrower than the transmit beam and:

$$\Delta R_g^r = \frac{\lambda R}{W^r \cos\theta_i} \tag{12}$$

which means that the PRF upper limit is much higher than for conventional SARs, for which W^t and W^r are equal. If the receive beam is narrow enough, and the beam shape controlled, then range ambiguities will only arise from areas of the receive beam that are very low down in the sidelobes.

Another constraint on the PRF for conventional SAR systems is that the duration of the return echo represented by the desired swath should be narrower than the Interpulse Period (IPP), so that the system is not configured to simultaneously transmit and receive at the same time. This can be expressed as:

$$IPP = (1/PRF) \geq \left(\frac{\lambda R \tan\theta_i}{cW^t \cos\theta_L} + 2\tau_p \right) \tag{13}$$

For SweepSAR systems, this constraint can also be relaxed, provided more than one receiver is available for simultaneous reception of return echoes from different portions of the illuminated swath. In a SweepSAR system, one could have, for example, two receive beams 'sweeping' over separate 100 km swaths, divided from each other by a window or 'gap' which represents the transmit pulse event. These gaps in swath coverage can be filled in by 'staggering' the PRF – adjusting it slightly in bursts, so the transmit event gap occurs at different locations across the swath for different azimuth looks, as suggested by Krieger et al in [17] and [18]. Depending on the actual implementation, this may result in a slightly degraded image quality for some portions of the swath.

The data rate for a SweepSAR system, is given by:

$$D_R \cong n_{chan} \left(\frac{\lambda R \tan\theta_i}{cW^t \cos\theta_L} + \tau_p \right) n_b f_s \, PRF \tag{14}$$

where n_{chan} is the number of receive channels, n_b is the number of bits used in digitization, and f_s is the sampling frequency (typically > twice the pulse bandwidth).

In the next section, we will explore two different design goals for a SweepSAR system. In both cases we will use configurations with $W^r > W^t$, so that the receive beam(s) are narrower than the transmit beam. The first design goal is to reduce the average transmit power (7) relative to a conventional SAR of antenna width W, keeping the swath width fixed. For this, we use:

$$W^t = W \text{ and } W^r > W \tag{15}$$

The second design goal is to maximize the illuminated swath width ΔR_g^t as in (8), allowing the average transmit power to vary. For this, we use:

$$W^t < W \text{ and } W^r = W \tag{16}$$

III. Design Examples

Consider a conventional SAR system with the characteristics summarized in Table I. This system is a planar array of dimensions 3.5 m by 13.5 m. As noted earlier, the average power on transmit shown in the table is calculated assuming a 100% orbital duty cycle, i.e. the radar is operating continuously.

	Stripmap Mode	Polarimetric Mode	ScanSAR Mode
Wavelength, λ	0.24 m		
Altitude, h	600 km		
Min. Incidence angle, θ_i(min)	17 deg		
Max. Incidence angle, θ_i(max)	43 deg		
Antenna length, L	13.5 m		
Antenna height, W	3.5 m		
Transmit power, P_t	5000 W	5000 W	5000 W
Pulse length, τ_p	60 μs	60 μs	60 μs
Average power on transmit, P_{av}	1050 W	2100 W	1050 W
Number of Rx channels, n_{chan}	1	2	2
Data rate, D_R	169 Mbps	373 Mbps	273 Mbps
Noise equivalent σ^o	-30 dB	-35 dB	-30 dB
Swath width, ΔR_{gg}	120 km	60 km	340 km
Spatial resolution, ρ	100 m	100 m	100 m
Number of looks	>100	> 100	>30

Table I: Design parameters for a conventional L-Band SAR system, illustrating three types of data acquisition: Stripmap, Polarimetric, and ScanSAR modes. To estimate the average power on transmit a DC-RF power conversion efficiency of 0.4 or 40% was assumed.

Table II shows the corresponding parameters for a similarly scoped SweepSAR system, designed to minimize the amount of DC power used on transmit as in (15). Wavelength, orbit altitude, and incidence angle range are the same as in Table I.

	Stripmap Mode	Polarimetric Mode	ScanSAR Mode
Antenna length, L	13.5 m		
Antenna height on transmit, W^t	1.3 – 1.8	2.6 – 3.6	1.3 – 1.8
Antenna height on receive, W^r	13.5	13.5	13.5
Transmit power, P_t	1200 W	1200 W	1200 W
Pulse length, τ_p	40 μs	60 μs	40 μs

Average power on transmit, P_{av}	168 W	500 W	168 W
Number of Rx channels, n_{chan}	1	2	2
Data rate, D_R	163 Mbps	373 Mbps	255 Mbps
Noise equivalent σ^o	-30 dB	-35 dB	-30 dB
Swath width, W_g	120 km	60 km	340 km
Spatial resolution, ρ	100 m	100 m	100 m
Number of looks	>100	> 100	>30

Table II: Design parameters for a SweepSAR system, illustrating three types of data acquisition: Stripmap, Polarimetric, and ScanSAR modes.

Comparing Tabels I and II, we see that one can achieve comparable performance using SweepSAR in each mode, but at significantly reduced peak and average transmit power levels.

Next consider a SweepSAR system, designed to achieve wider swaths while allowing the average transmit power to vary as in eq. (16). The wavelength, orbit altitude, and incidence angle assumed to produce the results in Table III are again identical to the values used in Table I.

Comparing Tables I and III, we see that in the latter case we have much wider swaths for both the stripmap and polarimetric modes. In fact the stripmap mode in Table III has as wide a swath as the ScanSAR mode in Table I, but with significantly more looks. This comes at the expense of an increased data rate, and the addition of a second receive channel. The stripmap mode in Table III achieves the same dual channel capability of the ScanSAR mode in Table I using SweepSAR, but at a significantly increased data rate and twice the number of receive channels. The average power values for both modes in Table III are again less than the comparable values in Table I by a factor of 2 or 3, but not as low as in Table II.

	Stripmap Mode	Polarimetric Mode
Wavelength, λ	0.24 m	
Altitude, h	600 km	
Min. Incidence angle, $\theta_i(min)$	20 deg	
Max. Incidence angle, $\theta_i(max)$	40 deg	
Antenna length, L	13.5 m	
Antenna height on transmit, W^t	0.45 – 0.65	0.9 – 1.4
Antenna height on receive, W^r	13.5	13.5
Transmit power, P_t	1600 W	3000 W
Pulse length, τ_p	60 μs	60 μs
Average power on transmit, P_{av}	336 W	1260 W
Number of Rx channels, n_{chan}	4	6
Data rate, D_R	882 Mbps	877 Mbps
Noise equivalent σ^o	-30 dB	-35 dB
Swath width, W_g	340 km	160 km
Spatial resolution, ρ	100 m	100 m
Number of looks	>100	> 100

Table III: Design parameters for an L-Band SweepSAR system, illustrating two types of wideswath data acquisition: Stripmap, and Polarimetric modes.

Finally, in Figures 3 and 4 we plot the SNR and ambiguity performance for SweepSAR stripmap and quad-pol modes, respectively. Similar (though not identical) parameters to those given in Table III were used to generate these plots. The data gaps that appear in each plot correspond to transmit events. The ambiguity levels plotted in Figs. 3 and 4 are relative (as is usual), and combine both range and azimuth ambiguities into one value for each ground range position relative to the nadir point (directly beneath the spacecraft). In our analysis we found that azimuth ambiguities tend to dominate the combined range ambiguity values, because the instantaneous swath on receive is so narrow.

IV. ummary and Discussion

We have seen in the above that the SweepSAR technique offers the potential for significant reductions in the transmit peak and average power required for a SAR system. This is achieved by making full use of the areal extent of a reflector antenna on receive. The SweepSAR technique can also be used to generate wideswath, high-resolution coverage – a significant improvement over conventional ScanSAR techniques [18]. The penalty is a higher data rate and an increase in the number of receivers needed to record the return echo. The elevated data rate is not as big a problem as it might appear initially: note that in the 30 years since Seasat launched downlink rates for LEO satellites have increased significantly – from ~85Mbps up to ~640 Mbps. In addition, analog-to-digital converters (ADCs) have increased in bandwidth from ~ 20 MHz to several GHz.

The SweepSAR approach discussed in this paper is under consideration for adoption as a mode of operation of the radar instrument on NASA's DESDynI mission [14]. It is also being considered as part of the joint studies ongoing between DLR and NASA/JPL of a Tandem-L mission [15]. The parameters used have been selected to match as closely as possible the image characteristics expected for those mission concepts.

The average power reductions projected for SweepSAR on DESDynI and Tandem-L should be even lower than given in Tables II and III, when one factors in the orbital duty cycle for the radar. Both DESDynI and Tandem-L have science objectives in the solid earth (geophysics), ecosystems, cryosphere and hydrology science disciplines. To meet these objectives requires data acquisitions primarily over the land surface areas of the Earth (with some polar sea ice and coastal ocean coverage added in). The Earth's land surface is about 31% of the total surface area, so adding in the sea ice and coastal ocean results in coverage requirements of roughly 35%, i.e. the radar will need to be activated ~35% of the time (or for 35 minutes in a 100 minute orbit). Referring back to Table II, this means that the average transmit power required for even the most demanding mode (quad-pol) is under 200W. For the stripmap and ScanSAR modes the value is under 60 W. Allowing 100W for the remaining electronics in the radar (a typical value) and assuming that the radar data acquisition is distributed evenly between the three available modes, the power required from the spacecraft power system for the radar instrument should be under 200W in total (≤ 600W during radar operation).

Both alternatives addressed in this paper for SweepSAR are attractive. Wide swath coverage with performance comparable with conventional stripmap SAR is highly desirable for DESDynI and Tandem-L applications. Payload power is a known cost driver in any space mission, so an approach that reduces the payload power needs by a factor of 4 or more has to be seen as significant. Lower power means a reduced power system on board the spacecraft, in particular smaller solar panels, and batteries, and the overall mass of the platform is reduced. When the lower mass of the reflector antenna (compared with the phased array) is also taken into consideration, a reflector+phased array SAR at L-band offers a very attractive solution.

References

[1] Curlander, J.C. and McDonough, R.N., 1991, *Synthetic Aperture Radar Systems and Signal Processing*, Wiley Series in Remote Sensing, John Wiley & Sons.

[2] Freeman, A.; Johnson, W.T.K.; Huneycutt, B.; Jordan, R.; Hensley, S.; Siqueira, P.; Curlander, J.; The "Myth" of the minimum SAR antenna area constraint, IEEE Transactions on Geoscience and Remote Sensing, Volume 38, Issue 1, Jan. 2000 pp. 320 - 324

[3] R. K. Moore, J. P. Claassen, and Y. H. Lin, "Scanning spaceborne synthetic aperture radar with integrated radiometer," IEEE Trans. Aerosp. Electron. Syst., vol. AES-17, no. 3, pp. 410–420, May 1981.

[4] A. Currie and M. A. Brown, "Wide-swath SAR," Proc. Inst. Elect. Eng., F, vol. 139, no. 2, pp. 123–135, Apr. 1992.

[5] Chang, C.Y., Jin, M. Y., Lou, Y-L., and Holt, B., First SIR-C Scansar Results**,** IEEE TGRS, Vol. 34, No. **5**, pp. 1278-1281, Sept. 1996

[6] T.G. Farr and M. Kobrick, "Mapping the World in 3-D: The Shuttle Radar Topography Mission", Pecoral4 Landsatellite Information 111, Denver, CO, Dec. 1999.

[7] Kretsch, J.L., Shuttle radar topography mission overview, Applied Imagery Pattern Recognition Workshop, 2000. Proceedings. 29th, pp. 276 – 282, Oct. 2000.

[8] De Zan, F. and Guarnieri, A. M., TOPSAR: Terrain Observation by Progressive Scans, IEEE TGRS, Vol. 44, No. 9, pp. 2352-2360, Sept. 2006

[9] Younis, M.; Wiesbeck, W., SAR with digital beamforming on receive only, Proc. IGARSS 1999, Vol. 3, pp. 1773 – 1775, 28 June-2 July 1999

[10] Younis, M., Fischer, C. and Wiesbeck, W. "Digital Beamforming in SAR Systems," *IEEE TGRS,* vol.41, no.71, pp. 1735-1739, July 2003

[11] Kim, J-H., Younis, M., and Wiesbeck, W., Implementation of Ground-based SAR demonstrator System for Digital Beam Forming, Proc. IGARSS 2005, Vol6, July 2005 pp. 4037 – 4040, 2005.

[12] Krieger, G., Gebert, N., and Moreira, A., Multidimensional Waveform Encoding: A New Digital Beamforming Technique for Synthetic Aperture Radar Remote Sensing, *IEEE TGRS*, Vol. 46, No. 1, Jan 2008.

[13] Heer, C. and Shutie, P. F., Digital Beam forming synthetic aperture radar, Microwave Symposium Digest, 2005 IEEE MTT-S International, June 2005.

[14] Freeman, A., et al, Deformation, Ecosystem Structure, and Dynamics of Ice (DESDynI), Proc. EUSAR 2008, Friedrichshafen, Germany, 2008

[15] Krieger, G., et al, The Tandem-L Mission Proposal: Monitoring Earth's Dynamics with High Resolution SAR Interferometry, Radarcon '09, Pasadena CA, 2009.

[16] Ramanujam, P., Law, P. H., Lane, S. O., Multi-beam reflector with a simple beamforming network, US Patent #6366256, 2000.

[17] Krieger G., Gebert N., Younis M., Moreira A., "Advanced Synthetic Aperture Radar Based on Digital Beamforming and Waveform Diversity", IEEE Radar Conference, Rome, Italy, pp. 767-772, May 2008.

[18] Krieger, G.; Gebert, N.; Younis, M.; Bordoni, F.; Patyuchenko, A.; Moreira, A., "Advanced Concepts for Ultra-Wide-Swath SAR Imaging", Proc. EUSAR 2008, Friedrichshafen, Germany, pp. 31-34, June 2008.

[19] Krieger, G.; Gebert, N.; Moreira, A., "Unambiguous SAR signal reconstruction from nonuniform displaced phase center sampling", IEEE Geoscience and Remote Sensing Letters, vol. 1, pp. 260-264, 2004.

[20] Gebert, N.; Krieger, G.; Moreira, A., "Digital beam-forming on receive: techniques and optimization strategies for high-resolution wide-swath SAR imaging", IEEE Trans. AES, in print 2008.

[21] G. D. Callaghan, I. D. Longstaff, "Wide-swath space-borne SAR using a quad-element array," IEE Proc. Radar Sonar Navig., vol. 146, pp. 159-165, 1999.

[22] H. Griffiths, P. Mancini, "Ambiguity suppression in SARs using adaptive array techniques," in Proc. IGARSS, Espoo, Finland, pp. 1015-1018, 1991.

[23] M. Suess, B. Grafmueller, R. Zahn, "A novel high resolution, wide swath SAR system," in Proc. IGARSS, Sydney, Australia, pp. 1013-1015, 2001.

[24] J. H. Blythe, "Radar Systems", US Patent 4,253,098, Feb. 1981.

[25] J.T. Kare, "Moving Receive Beam Method and Apparatus for Synthetic Aperture Radar", US Patent 6,175,326 B1, July 2001.

[26] M. Suess and W. Wiesbeck, "Side-looking synthetic aperture radar system," Eur. Patent EP 1 241 487 A 1, 2001.

Acknowledgements

Part of the work described here was performed at the Jet Propulsion Laboratory, California Institute of Technology, under contract with the National Aeronautics and Space Administration. The authors would like to thank their many colleagues at both JPL and DLR who contributed to the DESDynI and Tandem-L system design studies.

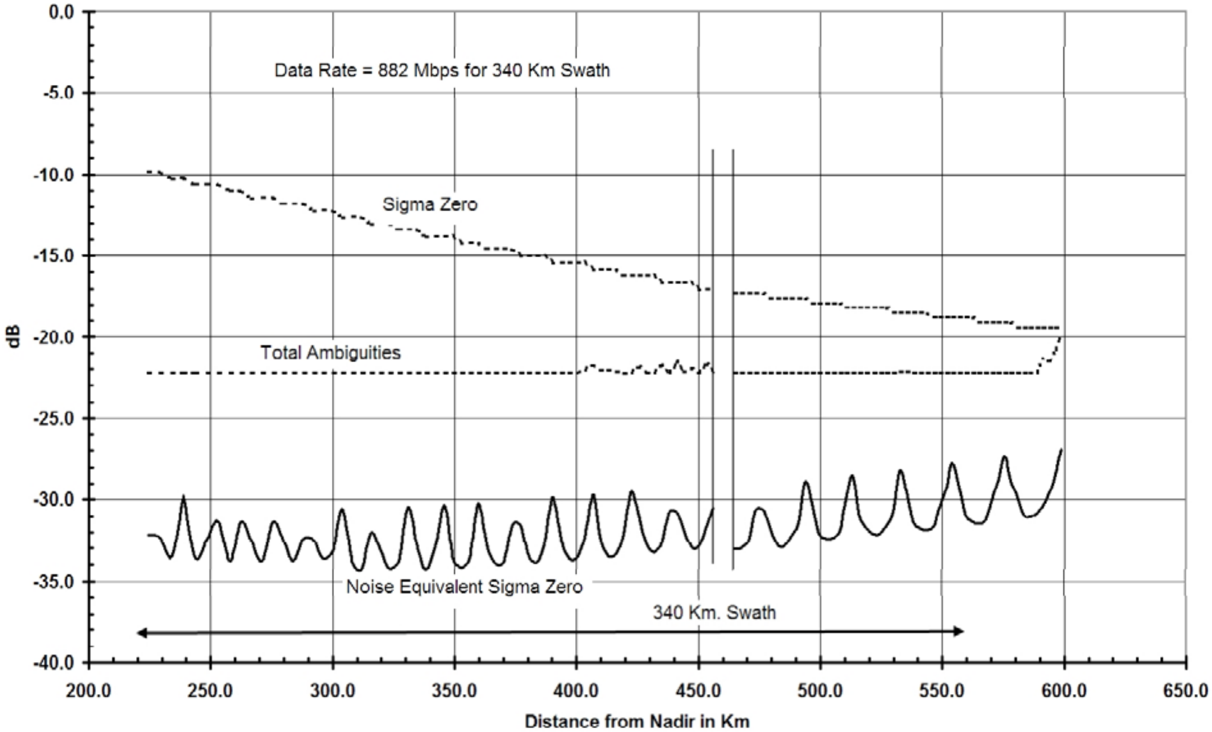

Figure 3: SweepSAR performance for the wideswath Stripmap mode similar to that in Table III, using idealized antenna patterns. Note the data gap in swath coverage, which corresponds to a transmit event. Either side of the 'data gap' separate receive beams are 'swept' across the swath, tracking the return echo. Each receive beam requires its own receiver, doubling the number of receive channels.

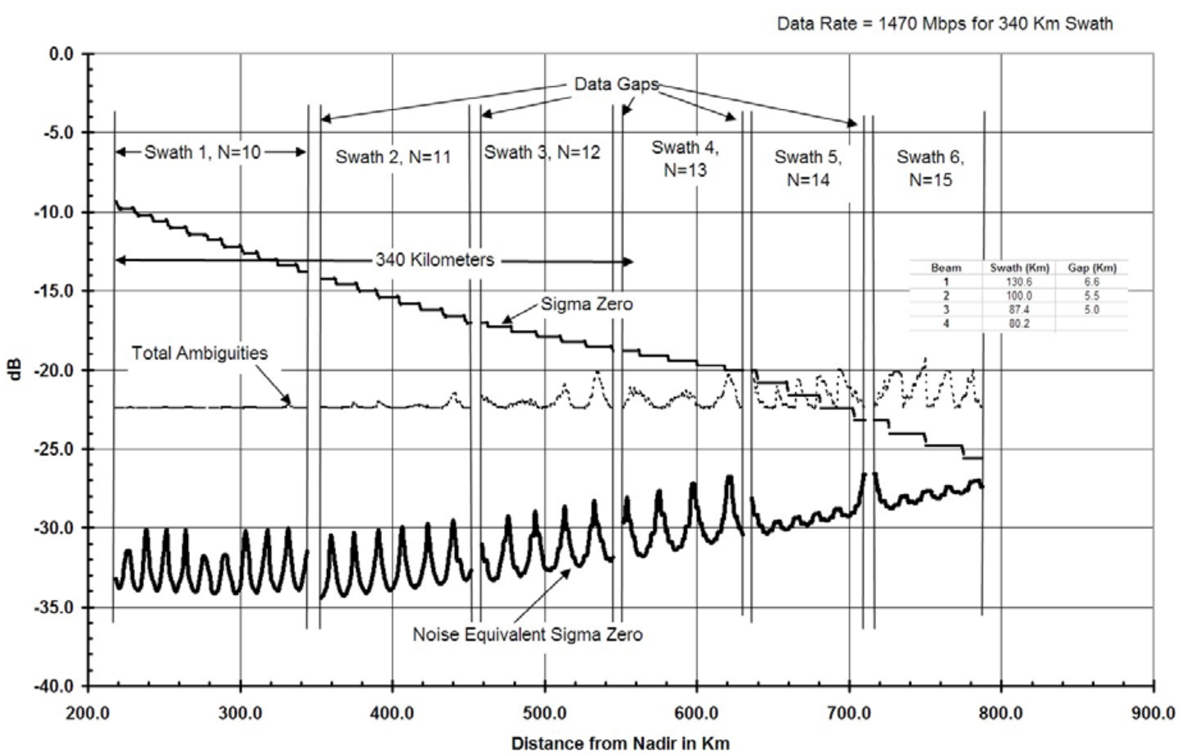

Figure 4: SweepSAR performance for the Quadpol mode similar to that in Table III, using idealized antenna patterns. Note the data gaps in swath coverage, which corresponds to transmit events. Either side of the 'data gaps' separate receive beams are 'swept' across the swath, tracking the return echo. Each receive beam require its own receiver, increasing the number of receive channels needed.